Articles

Electrostatic Contributions to Binding of Transition State Analogues Can Be Very Different from the Corresponding Contributions to Catalysis: Phenolates Binding to the Oxyanion Hole of Ketosteroid Isomerase†

Arieh Warshel,*,‡ Pankaz K. Sharma,‡ Zhen T. Chu,‡ and Johan Åqvist§

Department of Chemistry, University of Southern California, 418 SGM Building, 3620 McClintock Avenue, Los Angeles, California 90089-1062, and Department of Cell and Molecular Biology, Uppsala University, BMC, Box 596, SE-751 24 Uppsala, Sweden

Received August 24, 2006; Revised Manuscript Received October 26, 2006

ABSTRACT: The relationship between binding of transition state analogues (TSAs) and catalysis is an open problem. A recent study of the binding of phenolate TSAs to ketosteroid isomerase (KSI) found a small change in the binding energy with a change in charge delocalization of the TSAs. This has been taken as proof that electrostatic effects do not contribute in a major way to catalysis. Here we reanalyze the relationship between the binding of the TSAs and the chemical catalysis by KSI as well as the binding of the transition state (TS), by computer simulation approaches. Since the simulations reproduce the relevant experimental results, they can be used to quantify the different contributions to the observed effects. It is found that the binding of the TSA and the chemical catalysis represent different thermodynamic cycles with very different electrostatic contributions. While the binding of the TSA involves a small electrostatic contribution, the chemical catalysis involves a charge transfer process and a major electrostatic contribution due to the preorganization of the active site. Furthermore, it is found that the electrostatic preorganization contributions to the binding of the enolate intermediate of KSI and the TS are much larger than the corresponding effect for the binding of the TSAs. This reflects the dependence of the preorganization on the orientation of the *nonpolar* form of the TSAs relative to the oxyanion hole. It seems to us that this work provides an excellent example of the need for computational studies in analyzing key experimental findings about enzyme catalysis.

The origin of enzyme catalysis is a problem of great importance and significant current interest (e.g., refs *1*−*8*). Simulations and conceptual studies have suggested that electrostatic effects provide the major factor in enzyme catalysis (*2*, *9*, *10*) and that other factors cannot make large contributions (*2*). On the other hand, some workers believe that many effects have been exploited in the evolution of enzyme catalysis (e.g., refs *11* and *12*). Establishing the relative importance of different catalytic factors by direct experimental studies is very challenging, since such an analysis requires a decomposition of the observed energetic to different contributions, and in some cases, it is not clear how to overcome this challenge.

Nevertheless, recent work attempted just to resolve this challenging issue experimentally, focusing on estimating the electrostatic contribution to catalysis. That is, Kraut et al. (*11*) explored the effect of the oxyanion hole of ketosteroid isomerase (KSI)[1] by examining the energies of binding of series of phenolate ions to this site, considering these ions to represent good transition state analogues (TSAs). This study produced an interesting and instructive correlation between the binding energies of the phenolate ions and the delocalization of their hydrogen bonding (as estimated from NMR shifts) to the proton donors of the oxyanion hole. An attempt to use this correlation as an experimental tool in the assessment of the importance of electrostatic energies in enzyme catalysis was then made. The finding of a small change in binding energy for a significant change in delocalization was interpreted as evidence that electrostatic contributions do not play a major role in KSI and presumably in other enzymes.

In this work we will try to explore the actual information content in the experimental findings and illustrate that it is sometimes essential to use modern simulation approaches rather than conventional physicochemical assumptions in elucidating the catalytic significance of the phenolate binding

† This work was supported by Grant GM24492 from the National Institutes of Health (NIH) and the Swedish Research Council (VR).

* To whom correspondence should be addressed. E-mail: warshel@usc.edu. Phone: (213) 740-4114. Fax: (213) 740-2701.

‡ University of Southern California.

§ Uppsala University.

[1] Abbreviations: KSI, ketosteroid isomerase; EVB, empirical valence bond; FEP, free energy perturbation; LBHB, low-barrier hydrogen bond; AC, adiabatic charging; US, umbrella sampling; TSA, transition state analogue.

10.1021/bi061752u CCC: $37.00
Published on Web 01/17/2007

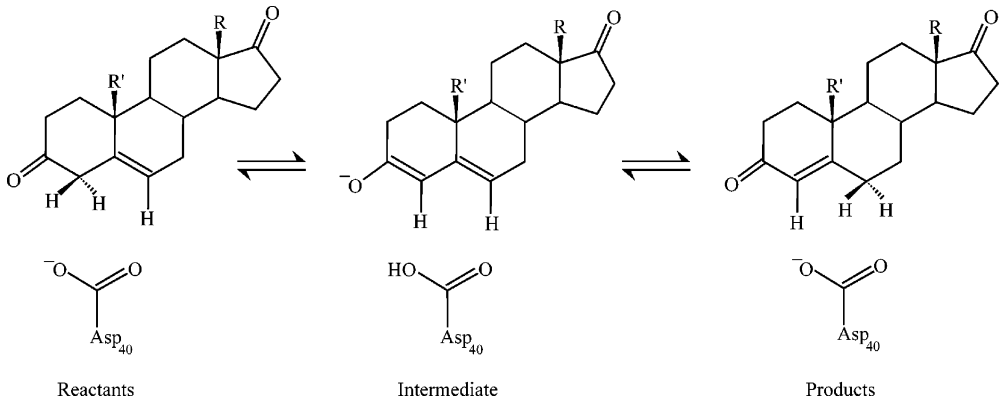

FIGURE 1: Schematic description of the catalytic reaction of KSI. This figure describes only the chemical parts of the system so that it can be compared conveniently to the corresponding reference reaction in water. The reaction is described in terms of the actual states rather than by arrows that correspond to electronic rearrangements.

experiments. It will be shown that the binding process of the TSAs involves a very small electrostatic contribution and a large contribution from the nonpolar interactions with the ligand. The chemical rate-determining step, on the other hand, involves a transfer of charge from Asp 40 to the oxygen of the enolate of the substrate, and this step involves a major electrostatic catalysis due do the preorganization of the enzyme active site. It will also be demonstrated that the electrostatic contribution to binding of the phenolates is very different from the corresponding contribution to the binding of the enolate intermediates of the reacting system (and the actual TS) and that this difference is associated with a major difference in the corresponding preorganization effect. This comparative study provides a clear illustration of the importance of electrostatic effects in enzyme catalysis.

The catalytic reaction of KSI is described schematically in Figure 1 (see refs *9* and *13*−*16* for more discussion). In this work, we will consider only the first step of the reaction, since the two steps are thought to have similar barriers in the enzyme and similar catalytic effects (*9*). Now, the first step in the chemical reaction of KSI involves a very large catalytic effect where the activation barrier for the reaction in solution ($\Delta g^{\ddagger}_{w}$) is ∼21.9 kcal/mol [correcting this for 55 M, which is roughly the cage effect of ref *1*, gives a $\Delta g^{\ddagger}_{cage}$ of ∼19.6 kcal/mol (*9*)], while the rate-determining barrier in the enzyme is ∼10.3 kcal/mol (*14*). Thus, the rate acceleration, $\Delta\Delta g^{\ddagger}$, is 11.6 kcal/mol. The origin of the catalytic effect has been attributed to the electrostatic stabilization of the enolate intermediate by the hydrogen bonds of Tyr 57 and Asp 103, described in Figure 2, and the reduction of the reorganization energy during the reaction (see ref *9*).

Some workers (e.g., ref *17*) have attributed the catalytic effect to a low-barrier hydrogen bond (LBHB) between the enolate and Tyr 57, but a careful EVB study by Feierberg and Åqvist (*9*) demonstrated that the catalytic effect is not due to LBHB but to the combined preorganization of the Tyr 57 and Asp 103 dipoles. There is also experimental evidence that the enolate is stabilized by these two hydrogen bonds rather than by a delocalized bond with Tyr 16 (e.g., ref *18*). At any rate, although the theoretical calculations of ref *9* strongly supported the electrostatic stabilization mechanism for KSI (see also ref *19* for experimental support), it is hard to establish this finding by direct experimental studies.

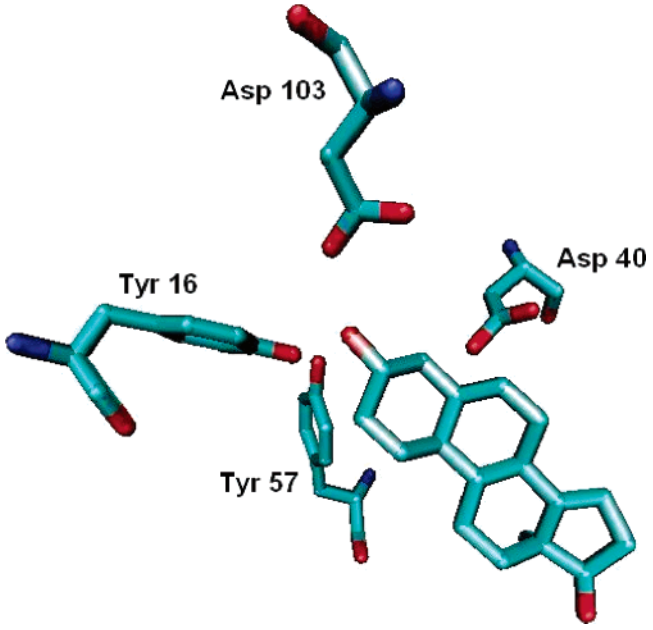

FIGURE 2: Substrate and key residues in the active site of KSI.

A recent attempt to determine the magnitude of the electrostatic contribution to the catalytic effect of KSI and in other oxyanions was reported by Kraut et al. (*11*). These workers evaluated the binding energies of different phenolate TSAs to KSI and observed a very small change in the binding energy with a change in the pK_a of the phenolates (due to different substituents). The observed trend in the binding energies was then used as a probe for the electrostatic contribution to catalysis. This was done by assuming that the electrostatic contribution to binding of a phenolate is correlated with the delocalization of the charge on the oxygen of the phenolate. Such an assumption is, however, quite problematic, since (a) the change in delocalization will also lead to a reduced level of solvation of the phenolate in water, (b) the degree of delocalization was deduced from the NMR shift, but this shift reflects the charge transfer to the tyrosine, and (c) the binding energy might not be related to the catalytic effect.

In our view, it is hard to explore the points mentioned above without careful theoretical studies, and this will be done in the subsequent sections. However, we emphasize that the idea that electrostatic effects play a major role in the catalytic effect of KSI is related to the chemical step

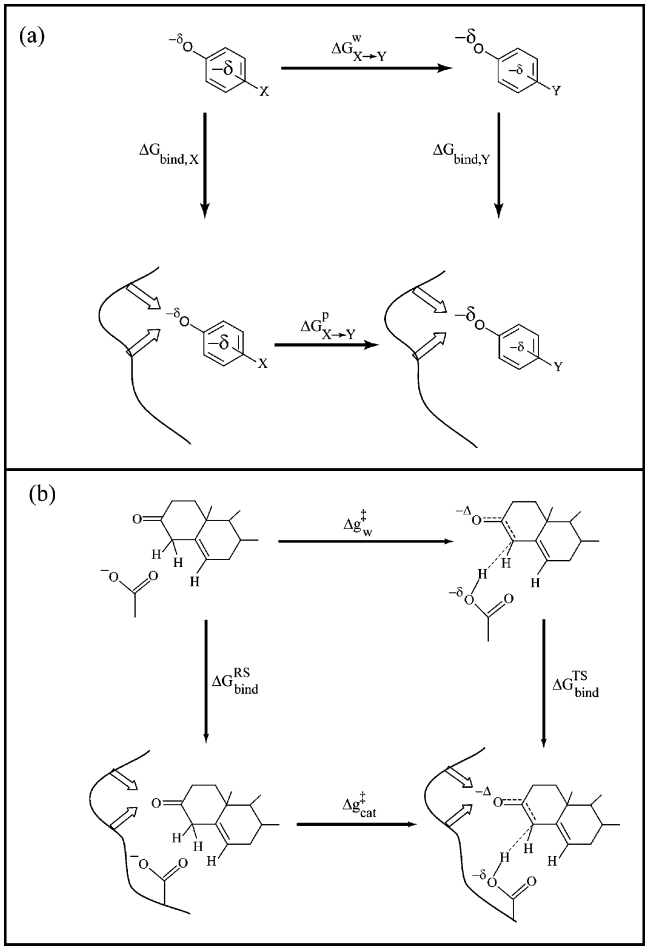

FIGURE 3: Thermodynamic cycles for (a) the binding of the phenolate TSA ligands and (b) the catalytic reaction of KSI. This figure draws attention to the fact that the cycles are not identical, although in some cases the electrostatic contributions to $\Delta g^{\ddagger}_{cat}$ can be similar to ΔG^{TS}_{bind}.

(which is characterized by k_{cat}, or more precisely by k_3) and not to the TS binding (which is related to k_{cat}/K_M) (*1*). Thus, it is useful to recognize that the binding of a TSA does not tell us directly about the electrostatic contribution to the chemical step, unless the ground state electrostatic contributions are negligible. That is, as shown in Figure 3, the binding cycle involves a transfer of a charge from water to the protein site, while the chemical process involves the very different transfer of a negative charge from Asp 40 to the steroid oxygen. The effect of the protein on these two processes is quite different. We also clarify that we do not question the usefulness of assessing binding energies of TSAs, but apparently this might not provide the best way of assessing electrostatic contributions to chemical catalysis. We also clarify that we will explore the binding of the TSAs and the TS.

COMPUTATIONAL METHODS

To analyze the energetics of the binding of the TSAs and the TS as well as the chemical catalysis, we have to consider both electrostatic and charge transfer contributions. At present, the most effective way of doing so is probably the use of the empirical valence bond (EVB) method (*1*, *20*, *21*), and this method will be used here. We clarify that the EVB does not involve any special focus on electrostatic contributions (although it evaluates them more reliably than most other methods), and it can capture any possible catalytic effect as has been demonstrated in our studies of almost any catalytic proposal [see discussion and references in a recent review (*2*)].

The use of the EVB will also be instrumental in separating electrostatic and nonelectrostatic charge transfer contributions. That is, in the EVB representation, we start with the charge distribution of the isolated reacting fragments and then let these zero-order charges interact with the surrounding environment and with each other. The mixing of the solvated charge states by the EVB off-diagonal terms allows us to quantify the charge transfer contributions.

The first step of our study involved the evaluation of the binding energy of the phenolates, using the cycles of Figure 3. The electrostatic parts of these cycles were evaluated by an adiabatic charging free energy perturbation (FEP) approach using the ENZYMIX force field (*22*). The charges for the phenolates were taken from the ab initio ESP (*23*) charges evaluated at the B3LYP/6-31+G* level using the GAUSSIAN03 (*24*) package for the given system in a COSMO solvent model (*25*, *26*). The relevant charges are given in Table 1 of the Supporting Information. We clarify at this point that obtaining the charges with a better quantum scheme is extremely unlikely to change any of our conclusions, since we always compare the solvation in water and in the protein active site, and this comparison makes the results relatively insensitive to the exact charges that are used. This point has been established in many of our papers (e.g., refs *27* and *28*).

The calculations of the reaction profile for the chemical step and charge transfer effects were performed using the EVB method and involved the three following diabatic states

$$\phi_1 = A^- H{-}D \quad H{-}Z$$
$$\phi_2 = A{-}H \quad D^- H{-}Z \qquad (1)$$
$$\phi_3 = A{-}H \quad D{-}H \quad Z^-$$

where A is the proton acceptor, D is the ketosteroid, and Z is a group that forms a hydrogen bond with the enolate (e.g., Tyr 16 in the protein and a water molecule in water) that can form, in principle, a delocalized hydrogen bond, which is also known by its common name, a low-barrier hydrogen

Table 1: Components of the Binding Energy of the Phenolate and Trifluorophenolate Ligands[a]

System	$\Delta G^{p}_{np\rightarrow ion}$	$\Delta G^{w}_{np\rightarrow ion}$	$\Delta G^{w\rightarrow p}_{np}$	ΔG^{p}_{CT}	ΔG^{w}_{CT}	ΔG_{bind}	ΔG^{obs}_{bind}	pK_a[b]
$\phi{-}O^-$	−83	−82	−7.0	−1.9	−1.0	−8.9	−10.5	9.95
$F_3\phi{-}O^-$	−73	−73	−8.3	−1.5	−1.0	−8.3	−10.3	7.10

[a] The different contributions are defined in Figure 4 and are given in kilocalories per mole. [b] The pK_a values are for the parent compounds, viz., phenol and 3,4,5-trifluorophenol.

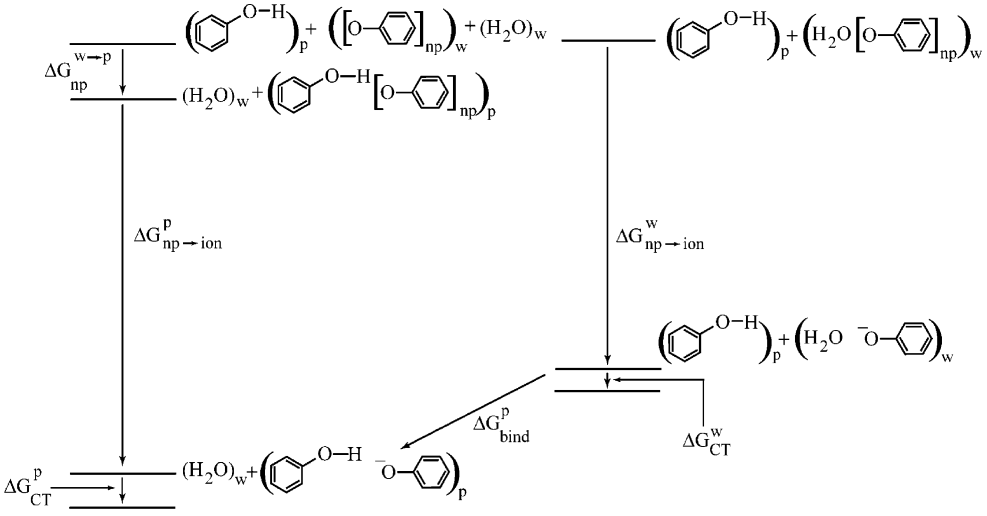

$$\Delta G_{bind} = \Delta G^{p}_{np\to ion} - \Delta G^{w}_{ion\to np} + \Delta G^{w\to p}_{np} + \Delta G^{p}_{CT} - \Delta G^{w}_{CT}$$

FIGURE 4: The cycle used for calculation of the binding energy of the phenolate ligands. The cycle involves charging the ligand in the protein and water ($\Delta g^{p}_{np\to ion}$ and $\Delta g^{w}_{np\to ion}$, respectively), the free energies of moving the nonpolar form of the ligand from water to the protein active site ($\Delta G^{w\to p}_{np}$), and the charge transfer or LBHB contribution in the protein active site and water (ΔG^{p}_{CT} and ΔG^{w}_{CT}, respectively). The charging step is illustrated by changing the ligand from being negatively charged to being completely nonploar (designated by a subscript np). The specific environment (water or protein) is designated by w or p, respectively.

bond (LBHB). The EVB free energy profiles were evaluated by the EVB free energy perturbation (FEP) umbrella sampling (US) mapping procedure, as described in detail elsewhere (*1*, *20*). The contributions to the binding free energies for the different phenolates were evaluated according to the cycle of Figure 4. The charging free energies, $\Delta G^{p}_{np\to ion}$ and $\Delta G^{w}_{np\to ion}$, were evaluated by using a standard adiabatic charging (AC) FEP procedure (e.g., refs *1* and *29*), changing the solute residual charges from zero to their values in the solution, $\mathbf{Q}^{s}_{S}$, in $m + 1$ incremental steps using

$$\mathbf{Q}_m = \mathbf{Q}^{s}_{S}\alpha_m \tag{2}$$

and

$$U_m = U(\mathbf{Q}_m)_{Ss} + U_{ss} \tag{3}$$

where U_{Ss} and U_{ss} are the solute−solvent and solvent−solvent potentials, respectively. With this, we have

$$\Delta\Delta G_{solv}(\alpha_m \to \alpha_{m+1}) = -RT \ln\langle \exp[-(U_{m+1} - U_m)/RT]\rangle_{U_m} \tag{4a}$$

$$\Delta G_{solv} = \sum_{m=1}^{n+1} \Delta\Delta G_{solv}(\alpha_m \to \alpha_{m+1}) \tag{4b}$$

The binding free energy of the nonpolar form of the ligands, ΔG_{np}, was evaluated by an FEP approach, which converts all the atoms of the nonpolar ligands to dummy atoms and shrinks the solute size at the same time to a small size. In addition to the free energy of this process, we also considered the entropic effect of moving the noninteracting substrate from the active site volume (v_{eff}) to a molar volume (v_0). The corresponding contribution is given by the relation $\Delta G = -RT \ln(v_0/v_{eff})$ (for more details, see the cycle of Figure 2 in ref *30*). Finally, we evaluated the charge transfer free energy, ΔG_{CT}, by applying the EVB approach to the system depicted in Figure 5 (see the Results and Discussion).

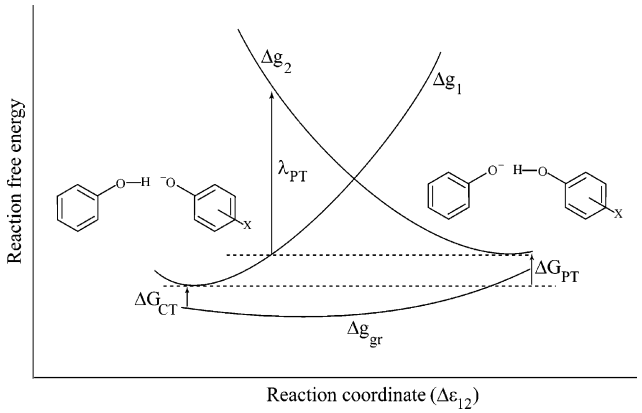

FIGURE 5: EVB description of the charge transfer contribution to the binding of the phenolates. This figure describes the diabatic surfaces for the case when the proton is on Tyr 16 (Δg_1) and on the phenolate (Δg_2). This figure also describes the ground state adiabatic free energy, Δg_{gr}. In the cases where the mixing term between the diabatic states is larger than the reorganization energy, one might have a delocalized hydrogen bond which will be stabilized by ΔG_{CT} relative to the electrostatic hydrogen bond.

The FEP/AC calculations were performed with 30 frames (i.e., 30 values of α_m in eq 2), each of 20 ps with time steps of 1 fs. These calculations were then repeated 10 times with different initial conditions, and the average value of all these calculations was taken as the calculated free energy. Before performing the simulations described above, we relaxed and equilibrated the simulation system with a 100 ps run. The EVB free energy profile (FEP/US) was evaluated in the same way as the FEP/AC calculations. The FEP/AC and FEP/US simulations were performed using the MOLARIS program package with an explicit simulation sphere of 18 Å completed to 21 Å by Langevin dipoles surface and then extended to infinity by a macroscopic sphere. This system was subjected to the SCAAS (*31*) surface constraints and the LRF long-

range treatment (*32*) and described by the ENZYMIX (*22*) force field. The reliability of the electrostatic simulations carried out using such a simulation protocol and the stability of such simulations to changes in the system size have been established in many of our studies (e.g., refs *33* and *34*). The ESP charges of Table 1 of the Supporting Information were used as the EVB charges. The EVB parameters used were the standard ENZYMIX parameters, except for the atoms involved in bond making and bond breaking. In this case, we adjusted the van der Waals parameters and the off-diagonal terms to reproduce the dependence of the ab initio energies and charges on the donor−acceptor distance (i.e., the results reported in Table 1 of the Supporting Information).

RESULTS AND DISCUSSION

The first step of our study involved the evaluation of the binding energies of the two TSAs, namely, a phenolate anion and a 3,4,5-trifluorophenolate ion. The calculations involve evaluation of all the terms in the cycle of Figure 4, where the overall binding energy is given by

$$\Delta G_{\text{bind}} = \Delta G^{\text{p}}_{\text{np}\rightarrow\text{ion}} - \Delta G^{\text{w}}_{\text{np}\rightarrow\text{ion}} + \Delta G^{\text{w}\rightarrow\text{p}}_{\text{np}} + \Delta G^{\text{p}}_{\text{CT}} - \Delta G^{\text{w}}_{\text{CT}} \quad (5)$$

where $\Delta G_{\text{np}\rightarrow\text{ion}}$ is the free energy of converting the nonpolar form of the ligand to its polar (or charged) form, $\Delta G^{\text{w}\rightarrow\text{p}}_{\text{np}}$ is the free energy of moving the nonpolar form of the ligand from water to the protein active site, and ΔG_{CT} is the free energy of allowing the charged ligand to form a nonelectrostatic delocalized charge transfer bond with possible proton donors. The specific environment (water or protein) is designated by w or p, respectively.

The different terms were evaluated as discussed in Computational Methods, and the corresponding results are summarized in Table 1. Note in this respect that the electrostatic term was calculated by running 10 AC-FEP calculations with different initial conditions, thus reducing possible convergence errors. As seen from Table 1, we reproduced the trend in the observed binding energies. In particular, it is significant to see that we reproduced the experimental finding of a small difference in binding energies of two phenolates with quite different pK_a values. It is also important to point out that the electrostatic contributions to the binding energy are very small in both the cases (<2 kcal/mol). This has, however, very little to do with the chemical catalysis. That is, it may be assumed by some that the fact that the binding energy and the chemical catalytic effect are around 10 kcal/mol means that the electrostatic contributions are similar (and thus small) in both cases. With this in mind, one might assume that the catalytic effect involves a small electrostatic contribution and thus, presumably, most of the catalytic effect is due to unspecified nonelectrostatic effects (*11*). However, this view (which was not stated in ref *11* but could be assumed by some readers) is very problematic, since most of the binding energy is due, in fact, to the nonpolar terms which simply do not exist in the chemical step (this point will be elaborated further below).

As stated above, calculations of the binding energies established that the small electrostatic contributions to these free energies cannot account for the very large catalytic effect of KSI. However, as discussed in the introductory part of the paper, the binding and the chemical cycles are very different and they can have very different electrostatic contributions. To demonstrate and quantify this issue, we evaluated the free energy profile of both the reaction of KSI and the corresponding reference solution reaction. Note in this respect that the catalytic effect in KSI is evaluated relative to a reference reaction in solution that includes an ionized aspartic acid as a general base. This approach, which is described in ref *2*, is based on the realization that the energetics of the general base is very well understood in terms of the pK_a values of the donor and acceptor and was never a part of the catalytic puzzle. At any rate, the calculated free energy profiles are given in Figure 6.

As seen from Figure 6, the calculated value of $\Delta g^{\ddagger}_{\text{cage}} - \Delta g^{\ddagger}_{\text{cat}}$ is ~8 kcal/mol so that $\Delta g^{\ddagger}_{\text{w}} - \Delta g^{\ddagger}_{\text{cat}} = 10.3$ kcal/mol. Thus, in agreement with a previous study (*9*), we reproduced the catalytic effect [$(\Delta\Delta g^{\ddagger}_{\text{calc}})^{\text{w}\rightarrow\text{p}} \cong 10$ kcal/mol, and $(\Delta\Delta g^{\ddagger}_{\text{obs}})^{\text{w}\rightarrow\text{p}} \cong 11.6$ kcal/mol] in a reasonable way. To demonstrate the electrostatic origin of this effect, we performed the EVB calculations while using zero residual charges for all the reacting atoms. The results of these calculations are summarized in Figure 7. As seen in Figure 7, the catalytic effect becomes zero when the electrostatic contributions are removed. Therefore, the electrostatic contribution to the chemical step is ~10 kcal/mol, and it accounts for almost all the observed effect, thus establishing our point about the chemical catalysis. We clarify in this regard that our calculations are not biased toward electrostatic effects in any shape or form, since the EVB surfaces represent all possible catalytic effects. We did not attempt to explore nuclear tunneling and dynamical effects in this work, since, as demonstrated in many of our previous studies, these effects are very similar in enzyme and in solutions, and we are not aware of any consistent experimental or theoretical study that established the importance of such effects in enzyme catalysis (e.g., see refs *35* and *36*). Furthermore, this study has been set up to explore the trend in electrostatic contributions.

In the next stage, we went one step further in comparing the binding of the TSA to the binding of the TS. That is, although as discussed in the introductory section, the binding of TSAs might not be directly related to chemical catalysis, it is crucial to demonstrate that even the binding of the TS and that of the TSA have very different electrostatic contributions. This point can be established by comparing the binding of the eneolate intermediate to that of the TSAs and then using the fact that the electrostatic contribution to binding of the eneolate is similar to that of the TS (see below). Thus, we used a FEP/AC approach, which transformed the charges of the enolate intermediate from zero to their actual value in both the protein active site and water. The corresponding calculated electrostatic contributions to binding of the enolate are summarized in Figure 8. As seen in Figure 8a, the electrostatic stabilization of the intermediate in the protein is larger by ~10 kcal/mol than the corresponding solvation in water. That is, one can see that at the beginning of the charging process ($\alpha = 0 \rightarrow \alpha = 0.15$), the energy of the bound intermediate decreases reasonably fast, while the energy in water stays around zero. This reflects the preorganization effect of the protein, since in the active site the protein dipoles are already oriented toward the

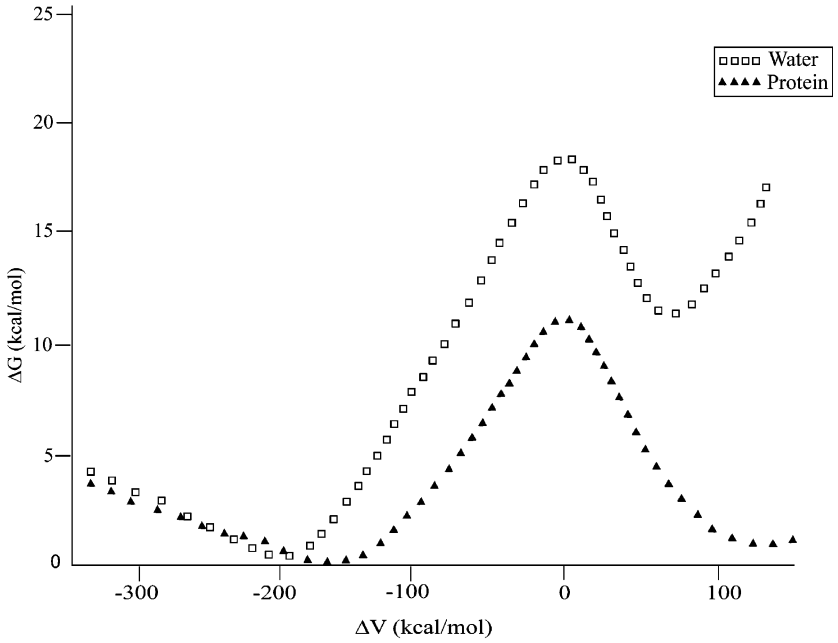

FIGURE 6: Free energy surfaces for the reaction of KSI (▲) and the corresponding reference reaction in water (□). This figure shows that the EVB calculations reproduced the catalytic effects since the TS in the protein (relative to the RS) is ~10 kcal/mol lower than the TS in water.

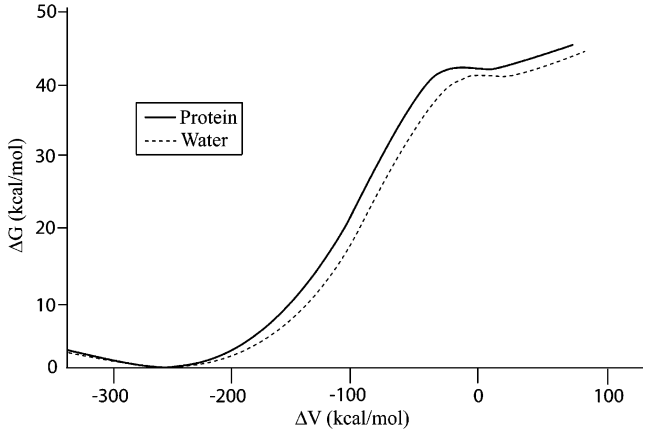

FIGURE 7: Free energy surfaces for the reaction of KSI (—) and the corresponding reference reaction in water (- - -) for the case where the residual charges of the reacting atoms are set to zero. This figure shows that the reduction of the chemical barrier is due to electrostatic effects.

developing charge while in water they are oriented randomly around the nonpolar form of the enolate. This effect is also illustrated in Figure 8b for the phenolate. As is clear from the figures, the fact that the enolate is more stable in the protein than in water is almost entirely associated with the preorganization effect. Interestingly, and very significantly, the preorganization effect is smaller in the case of binding of the phenolate TSA (shown in Figure 8b), and it does not compensate for the larger electrostatic energy in the charged state. This point is also illustrated in Table 2, where we present the results of the linear response approximation (LRA) (*30*) for both the enolate intermediate and the binding of the phenolate. This approach approximates the charging free energy as

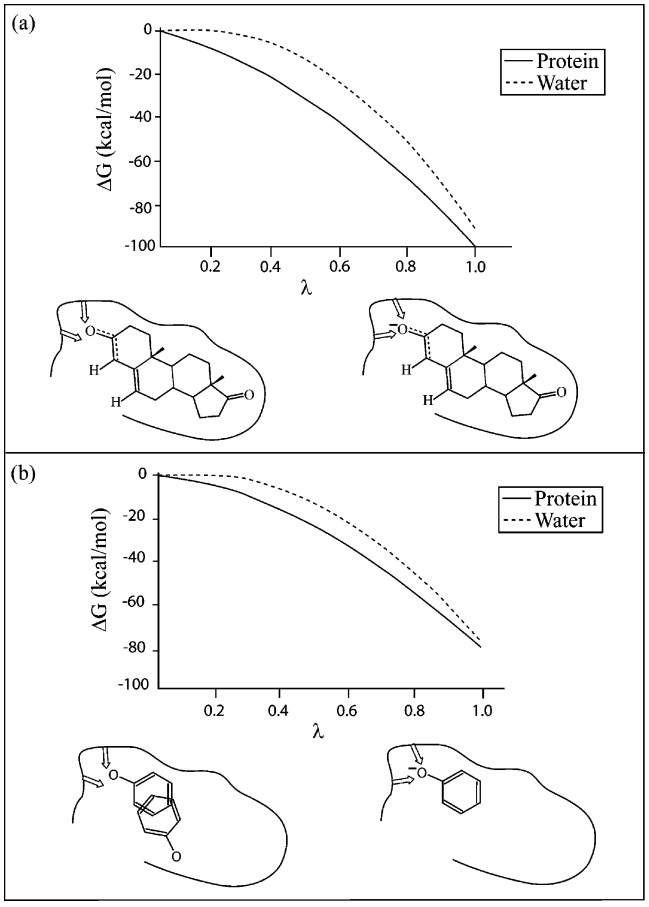

FIGURE 8: (a) Energetics of charging the enolate intermediate in the site of KSI and in water. (b) Energetics of charging the phenolate ligand in the active site of KSI. The bottom part of each figure also illustrates the preorganization effect, showing that this effect is significantly smaller in the case of the phenolates, since the ligand is not held in a fixed orientation once it is converted to its nonpolar form (see text).

Table 2: LRA Analysis for the Enolate and the Phenolate[a]

	enolate^w	enolate^p	phenolate^w	phenolate^p
$\langle U_Q - U_0\rangle_Q$	−209	−167	−179	−130
$\langle U_Q - U_0\rangle_0$	24	−36	13	−16
ΔG_{LRA}	−93	−102	−83	−73
ΔG_{FEP}	−92	−102	−75	−75

[a] The different LRA contributions (eq 6) are given in kilocalories per mole. As seen here, the preorganization term, $\langle U_Q - U_0\rangle_0$, is most negative for the enolate case. This term is not zero for the water case, due to the arbitrary selection of the solute system.

$$\Delta G_{np\rightarrow ion} \cong {}^1/_2[\langle U_Q - U_0\rangle_Q + \langle U_Q - U_0\rangle_0] \qquad (6)$$

where U_Q and U_0 are the potential energies of the nonpolar and polar (charged) forms of the ligand, respectively, while $\langle\ \rangle_Q$ designates an average over trajectories with the indicated charged form. The term, $\langle\ \rangle_0$, reflects the preorganization effect, which is zero when we deal with the ligand in solution (see ref *2*). As seen from the table, the preorganization contribution is significantly larger in the case of the binding of the real intermediate than in the binding of the phenolate. This seems to be very significant and reflects the shape of the substrate that prevents its rearrangement in its nonpolar form. Since it is very hard to quantify experimentally the electrostatic component in the structures obtained upon binding of the nonpolar form (the $\langle U_Q - U_0\rangle_0$ term), it is very important to have the corresponding theoretical result. In this respect, it would be interesting to explore binding of ligands that resemble the actual intermediate better. It is also important to realize that the electrostatic contributions of the binding of the enolate intermediate are similar to the corresponding contributions to the binding of the TS. This point was established in a preliminary study that considered the charging of the actual TS. Since the polar preorganization concept may not be entirely familiar to some readers and is clearly not fully intuitive, we expand it by considering Figure 9. As seen here, the overall charging process can be decomposed into two steps: (a) charging the substrate (solute) while keeping the solvent (environment) in the orientation it had when the system was uncharged and (b) allowing the solvent to rearrange when the solute is already charged. The first term represents the preorganization effect, which is zero in water since the solvent is randomly oriented when the solute is uncharged.

Another interesting issue is the contribution of the so-called low-barrier hydrogen bond (LBHB) to catalysis and binding. This type of contribution is usually related to a catalytic proposal, where it is suggested that a delocalization effect (the charge transfer term, ΔG_{CT}, of eq 5) is larger in the protein than in solution and thus contributes in a major way to catalysis (see the definition and discussion in ref *37*). In general, it has been shown by careful EVB calculations (*37*, *38*) and by ab initio QM/MM calculations (e.g., refs *39* and *40*) that the LBHB effects are very small or even anticatalytic. Nevertheless, it is important to examine possible LBHB contributions; this was done here using the EVB approach, and the corresponding results are included in Tables 1 and 2. As seen from the tables, the CT contributions to binding are small but not negligible. Interestingly, these LBHB binding effects follow the relationship (*37*)

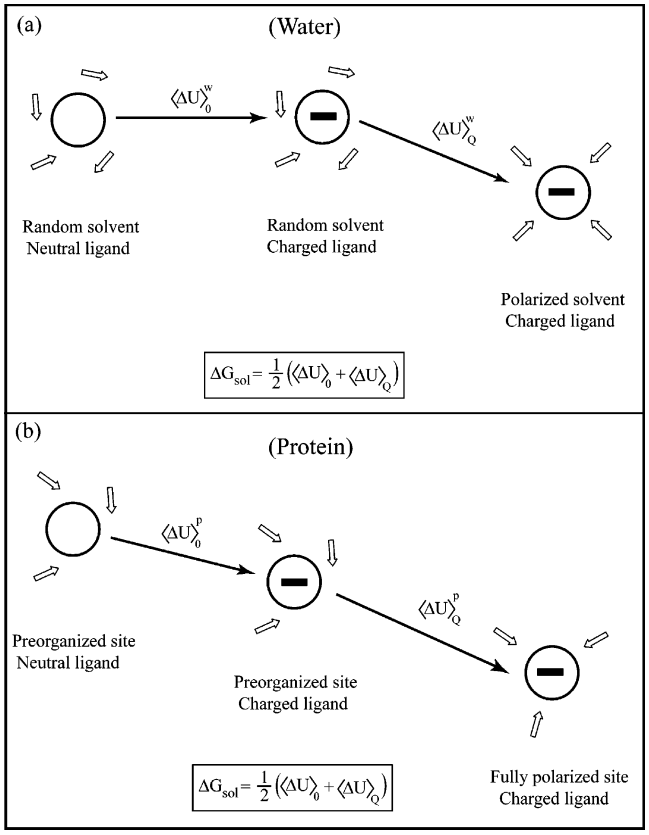

FIGURE 9: Demonstrating the preorganization effect by considering the stabilization of an ion in water by polarization effects (a), and the stabilization of an ion in a protein by the cumulative effects of polarization and preorganization (b) (see also text).

$$\Delta G_{CT} = -H_{12}^2/(\Delta G_{PT} + \lambda_{PT})$$
$$= -H_{12}^2/[2.3R(\Delta pK_a) + \lambda_{PT}] \qquad (7)$$

where ΔG_{PT} is the proton transfer energy defined in Figure 5, while ΔpK_a is the difference between the pK_a values of the phenolate and the proton donor (Tyr or H_2O) at the given environment. λ_{PT} is the reorganization energy, defined in Figure 5. Interestingly, the origin of the dependence of the LBHB energy on the pK_a is quite different from what has been proposed in ref *41* (see the discussion in ref *37*). Nevertheless, the weak dependence of the observed binding energy on the pK_a's of the phenolates indicates that we do not have a large LBHB contribution.

Equally interesting is the issue of the LBHB contribution to the catalytic effect of KSI (e.g., ref *42*). The earlier study of Feierberg and Åqvist (*9*) found that the LBHB contribution does not constitute a major catalytic factor. The work presented here found that the LBHB contribution ($\Delta G_{CT}^p - \Delta G_{CT}^w$) to the enolate binding is around −2 kcal/mol, as compared to the electrostatic contribution of −10 kcal/mol.

The overall contributions to binding of the TSA and to the binding of the eneolate intermediate as well as the chemical step are summarized in Figure 10. The main point that emerges is that we could reproduce the observed energetics while demonstrating that the electrostatic contribution to the TSA binding is not related to the corresponding contribution to catalysis or the contribution to the TS binding.

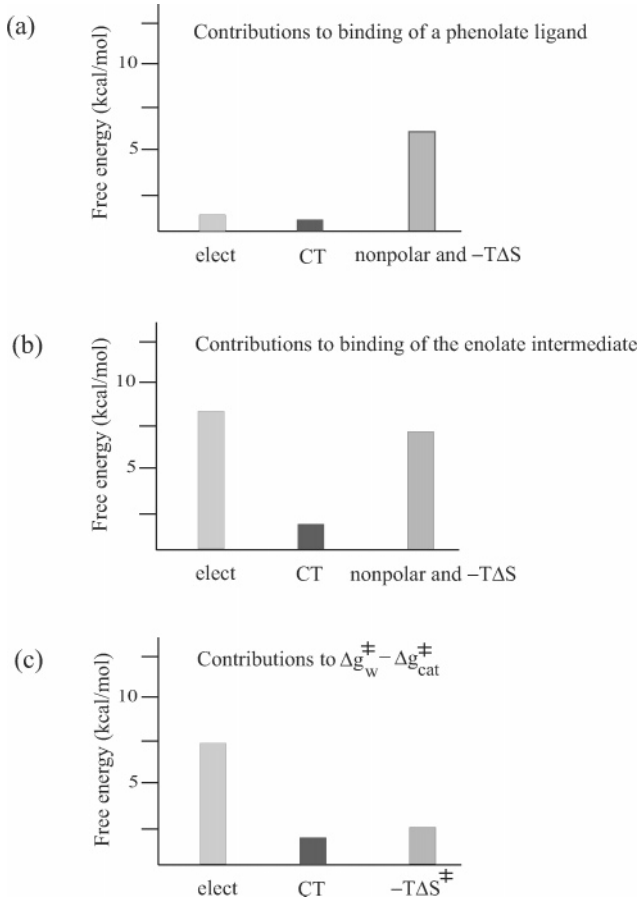

FIGURE 10: Free energy contribution to the binding of a phenolate ligand (a), to the binding of the enolate (b), and to $\Delta g^{\ddagger}_{w} - \Delta g^{\ddagger}_{cat}$ (c). The $-T\Delta S^{\ddagger}$ contribution in panel c reflects the cage contribution.

CONCLUDING REMARKS

Although there is a growing body of evidence which shows that the main catalytic factor of an enzyme is associated with electrostatic effects (see ref *2* for a review), it is hard to quantify these contributions by direct experimental studies. An interesting attempt to examine the electrostatic proposal, advanced recently (*11*), has evaluated the binding energy of different phenolate TSAs to KSI and considered the trend in this binding energy as a probe for the electrostatic contribution to catalysis. It was assumed that the electrostatic contribution to binding of the TSAs is correlated with the delocalization of the charge on the oxygen of the phenolate and, presumably, with the catalytic effect. Although the charge delocalization cannot be used as a quantitative yardstick for the electrostatic contribution to binding (see below), it does provide a useful qualitative probe for the interaction between the ionized form of the TSA and the protein. However, as demonstrated in this work (see also below), this interaction energy does not tell us about the preorganization effect, which is very different in the binding of the TSAs and the chemical processes and is also very different in the case of the binding of the actual high-energy reaction intermediate (the enolate) and the phenolate TSAs.

It seems to us that the best way to actually assess the relevance of the TSA binding experiments to the catalytic effect is to use some form of computer modeling approach that evaluates both the binding energy of the TSAs and the catalytic effect. This work calculated the electrostatic contribution to the binding of different phenolates to KSI and examined the relationship between these small contributions and the large electrostatic contribution to the chemical catalysis of KSI. The initial part of our analysis focused on the origin of the trend in the experimentally observed binding energy, and the calculation reproduced the finding that there is only a small change in the binding free energy despite significant changes in the pK_a values of the phenolates. The fact that the calculations reproduced the observed results indicates that they can be used to provide a detailed analysis of the origin of these results.

Several important points emerged from our analysis. First, it was found that the change in the charge localization of the phenolates cannot be used as a reliable probe for the magnitude of the electrostatic effect in the protein, since the change in delocalization also changes the solvation in water and since the predicted delocalization is quite different from the charge distribution evaluated by the quantum mechanical calculations. Second, the overall electrostatic contribution to binding is quite small and has very little relationship to the large electrostatic contribution to catalysis (see below). Furthermore, most of the contribution comes from the part of the cycle that considers the binding of the nonpolar form of the ligand. Finally, the delocalization as reflected by the NMR chemical shifts observed in ref *11* is mainly related to the charge transfer between the phenolate and Tyr 16 and not to the delocalization of the charge in the phenolate. Despite these problems, we can state that careful theoretical analysis that reproduced the observed binding energies agrees with the suggestion of ref *11* that the electrostatic contributions to binding are small. However, this analysis also demonstrates that the overall binding energy has little to do with the chemical catalysis, since most of the binding energy is due to the nonpolar contribution that plays no role in the chemical step.

Some workers may be inclined to assume that the binding energy of the TSAs is related to the chemical catalysis, since both energies are ~10 kcal/mol. However, as illustrated in this work, the main contribution to the TSA binding energy is due to the nonpolar term, but this term is basically zero in the chemical cycle. In other words, despite the problems with the analysis of Kraut et al. (*11*) mentioned above, it is true that the electrostatic contributions to the binding of phenolates to KSI are small. Unfortunately, the electrostatic contributions to binding do not allow us to estimate the electrostatic contributions to the chemical catalysis of the real substrate. To illustrate this problem, we evaluated the catalytic effect in the reaction of KSI. As found in the calculations and in a previous study (*9*), the large catalytic effect (~10 kcal/mol) can be reproduced in a quantitative way and is almost entirely due to electrostatic effects. This is demonstrated, for example, in Figure 7, where we compared the calculated reaction profile with and without solute−solvent electrostatic interactions. As seen from Figure 7, the free energy profiles in the enzyme and solution are very similar to each other when we turn off the solute−solvent electrostatic interactions. However, the barrier for the enzyme reaction is reduced by 10 kcal/mol when the electrostatic interactions are turned on (Figure 6). The difference between the catalytic reactions to the binding process is, in fact, a very profound difference. In the actual

reaction, we have a charge transfer from Asp 40 to the steroid oxygen (Figure 1) and reducing the reorganization energy in this process can have a major catalytic advantage. Also, the charge transfer process does not involve any significant change in the interaction between the enzyme and the uncharged form of the reacting system (it is very similar for the reactant and product state). On the other hand, the TSA binding process does involve a large $\Delta G_{np}^{w\rightarrow p}$.

In addition to the fact that the TSA binding and the chemical catalytic processes are different, there is a fundamental difference in the seemingly similar process of binding of the enolate intermediate and the binding of the phenolate ligands. As found here, the electrostatic preorganization effect is much larger in the case of the enolate intermediate of the real reacting system than the binding of the phenolates. This situation is explained with the help of Figures 8 and 9, where we illustrate the fact that a large preorganization effect requires the nonpolar form of the ligands or the intermediate to be oriented in the correct way, where the oxygen is pointing out toward the oxyanion hole (in addition to the requirement that the oxyanion hole be polarized toward the oxygen in the absence of charge on this oxygen). Apparently, the phenolates can easily rotate in the active site when they are in their nonpolar form. On the other hand, the real substrate is held in the correct orientation even in its polar form. It is important to note in this respect that the effect described above is fundamentally different from the so-called entropy trap (*43*), which is related to the entropy of aligning the reacting fragments (in this case Asp 40 and the steroid), rather than with aligning the fragments with respect to their surroundings (*44*). Apparently, in our case, we may have additional confusion regarding the possible extension of the entropy trap proposal to the orientation of the substrate relative to the protein groups. This entropic effect, which is approximately RT ln 2 (<1 kcal/mol), is trivial, since we are talking about 8 kcal/mol of electrostatic effects here. This possible confusion may arise due to the fact that it is simpler to understand the idea of rotation of the phenolates than the fundamental catalytic effect, which is the difference between the rotation (reorganization) of the water molecules on the way to the transition state in the solution reaction and having fixed dipoles in KSI. In other words, KSI catalysis should be considered relative to the reference reaction in water and not by comparing the binding of the phenolate and enolate.

In view of the findings in this work and ref *9*, it is important to clarify that the discussion of the reorganization effect in ref *11* reflects some misunderstanding. That is, the preorganization idea reflects fully quantitative considerations, which are now well accepted in the electron transfer community (e.g., ref *45*), and is not related to the number of water molecules or to the inability of some continuum models to evaluate this effect. At present, it appears that only microscopic computational approaches can quantify the preorganization contribution, and of course, the same models must be validated by reproducing the actual observed binding and catalysis.

The finding that the preorganization effect is much larger for the enolate of the true substrate than for the phenolates presents a challenge for experimental studies, where it would be interesting to see a dramatic increase in the binding energy of ligands that resemble the shape of the enolate. However, even in the absence of such a direct experiment, we can use a simple thermodynamic cycle and compare the transition state free energy, $\Delta g_p^{\ddagger}$, that corresponds to k_{cat}/K_M (or, more precisely, the rate of the chemical step divided by K_D) to the activation free energy in water, $\Delta g_w^{\ddagger}$ (see the discussion in ref *2*). With a $\Delta g_p^{\ddagger}$ value of ~3.0 kcal/mol (using a k_3 of 1.7×10^5 s^{-1} and a K_D of 5 μM; see refs *14*, *15*, and *18*) and a $\Delta g_w^{\ddagger}$ of 21.9 kcal/mol, we obtain the transition state binding free energy of ~19 kcal/mol as compared to only ~10 kcal/mol for the phenolates. Since, according to our calculations, the binding energies of the enolate intermediate and the actual transition state are similar, we can conclude that the binding energy of the enolate is ~17−19 kcal/mol, which is quite impressive. This binding energy has been obtained by our calculations that combined an ~10 kcal/mol electrostatic and CT effect with ~7 kcal/mol contributions from the nonpolar part of the cycle (see Figure 10).

The fact that the factors that contribute to binding energies can be very different from those involved in catalysis has several interesting implications. For example, some estimates of the ability of an enzyme to stabilize the transition state have been based on binding energies (*46*). However, ref *2* argues that such estimates are not fully justified. The present work provides further support to the idea that the factors involved in reducing $\Delta g_{cat}^{\ddagger}$ are frequently very different from those involved in the binding process.

The conclusions given above are also relevant to the concept of using TSA-type haptens to induce the formation of catalytic antibodies (*47*, *48*). As demonstrated in ref *49*, the charge distributions of the TSAs are usually quite different from those of the corresponding transition state. This finding is consistent with our finding, in pointing out the difference between the binding and catalytic processes.

It might be useful to comment here on the perception that the catalytic effect is due to many factors (e.g., ref *11*). While this possibility should always be considered, it is essential to define, examine, and quantify each proposed catalytic contribution, as done repeatedly in our studies (e.g., ref *2*). Now, while ref *11* does not clarify or quantify the nature of the presumed nonelectrostatic factors that can be examined computationally, it concludes that electrostatic effects do not play a crucial role. In this respect, it is important to consider key experiments, such as the effects of mutation of Try 16 and Asp 103, and ask what other catalytic effects, except electrostatic contribution, can account for the enormous effect of these residues. Here we can only point out that a previous study (*9*) found that the mutational effects are due to electrostatic interactions, and it is very hard to account for such effects by other catalytic factors.

Perhaps the most interesting conclusion from this work is the finding that the catalytic effect is almost entirely due to electrostatic preorganization effects. This trend that has been found in other enzymes (e.g., see the summary in ref *2*) indicates that enzyme catalysis is associated mainly with electrostatic factors rather than with many other small effects. Furthermore, the work reported here demonstrates the crucial role of computer simulations in converting the overall observed energetics to individual energy contributions to binding and catalysis.

ACKNOWLEDGMENT

We thank the High Performance Computing Center (HPCC) at the University of Southern California for computer time.

SUPPORTING INFORMATION AVAILABLE

One table of data comprising of energies and charges for different complexes of phenolates and a proton donor in the gas phase and in solution. This material is available free of charge via the Internet at http://pubs.acs.org.

REFERENCES

1. Warshel, A. (1991) *Computer Modeling of Chemical Reactions in Enzymes and Solutions*, John Wiley & Sons, New York.
2. Warshel, A., Sharma, P. K., Kato, M., Xiang, Y., Liu, H., and Olsson, M. H. M. (2006) Electrostatic basis for enzyme catalysis, *Chem. Rev. 106*, 3210−3235.
3. Borman, S. (2004) Much Ado About Enzyme Mechanisms, *Chem. Eng. News 82*, 35−39.
4. Fersht, A. (1999) *Structure and Mechanism in Protein Science. A Guide to Enzyme Catalysis and Protein Folding*, W. H. Freeman and Company, New York.
5. Bugg, T. D. H. (2001) The Development of Mechanistic Enzymology in the 20th Century, *Nat. Prod. Rep. 18*, 465−493.
6. Field, M. (2002) Stimulating Enzyme Reactions: Challenges and Perspectives, *J. Comput. Chem. 23*, 48−58.
7. Gao, J., and Truhlar, D. G. (2002) Quantum Mechanical Methods for Enzyme Kinetics, *Annu. Rev. Phys. Chem. 53*, 467−505.
8. Agarwal, P. K., Billeter, S. R., Rajagopalan, P. T. R., Benkovic, S. J., and Hammes-Schiffer, S. (2002) Network of coupled promoting motions in enzyme catalysis, *Proc. Natl. Acad. Sci. U.S.A. 99*, 2794−2799.
9. Feierberg, I., and Åqvist, J. (2002) The Catalytic Power of Ketosteroid Isomerase Investigated by Computer Simulation, *Biochemistry 41*, 15728−15735.
10. Ranaghan, K. E., and Mulholland, A. J. (2004) Conformational effects in enzyme catalysis: QM/MM free energy calculation of the 'NAC' contribution in chorismate mutase, *Chem. Commun.*, 1238−1239.
11. Kraut, D. A., Sigala, P. A., Pybus, B., Liu, C. W., Ringe, D., Petsko, G. A., and Herschlag, D. (2006) Testing Electrostatic Complementarity in Enzyme Catalysis: Hydrogen Bonding in the Ketosteroid Isomerase Oxyanion Hole, *PLoS Biol. 4*, 0501−0519.
12. Li, G. H., and Cui, Q. (2003) What is so special about Arg 55 in the catalysis of cyclophilin A? Insights from hybrid QM/MM simulations, *J. Am. Chem. Soc. 125*, 15028−15038.
13. Li, Y. K., Kuliopulos, A., Mildvan, A. S., and Talalay, P. (1993) Environments and Mechanistic Roles of the Tyrosine Residues of Δ^5-3-Ketosteroid Isomerase, *Biochemistry 32*, 1816−1824.
14. Hawkinson, D. C., Pollack, R. M., and Ambulos, N. P., Jr. (1994) Evaluation of the Internal Equilibrium Constant for 3-Oxo-Δ^5-steroid Isomerase Using the D38E and D38N Mutants: The Energetic Basis for Catalysis, *Biochemistry 33*, 12172−12183.
15. Mildvan, A. S., Weber, D. J., and Kuliopulos, A. (1992) Quantitative Interpretations of Double Mutations of Enzymes, *Arch. Biochem. Biophys. 294*, 327−340.
16. Schwab, J. M., and Henderson, B. S. (1990) Enzyme-Catalyzed Allylic Rearrangements, *Chem. Rev. 90*, 1203−1245.
17. Zhao, Q. J., Abeygunawardana, C., Talalay, P., and Mildvan, A. S. (1996) NMR evidence for the participation of a low-barrier hydrogen bond in the mechanism of Δ^5-3-ketosteroid isomerase, *Proc. Natl. Acad. Sci. U.S.A. 93*, 8220−8224.
18. Brooks, B., and Benisek, W. F. (1994) Mechanism of the Reaction Catalyzed by Δ^5-3-Ketosteroid Isomerase of *Comamonas* (*Pseudomonas*) *testosteroni*: Kinetic Properties of a Modified Enzyme in Which Tyrosine-14 Is Replaced by 3-Fluorotyrosine, *Biochemistry 33*, 2682−2687.
19. Petrounia, I. P., Blotny, G., and Pollack, R. M. (2000) Binding of 2-naphthols to D38E mutants of 3-oxo-Δ^5-steroid isomerase: Variation of ligand ionization state with the nature of the electrophilic component, *Biochemistry 39*, 110−116.
20. Aqvist, J., and Warshel, A. (1993) Simulation of Enzyme Reactions Using Valence Bond Force Fields and Other Hybrid Quantum/Classical Approaches, *Chem. Rev. 93*, 2523−2544.
21. Warshel, A., and Florian, J. (2004) The Empirical Valence Bond (EVB) Method, in *The Encyclopedia of Computational Chemistry* (von Ragué Schleyer, P., Allinger, N. L., Clark, T., Gasteiger, J., Kollman, P. A., Schaefer, H. F., III, and Schreiner, P. R., Eds.) John Wiley & Sons, Chichester, U.K.
22. Lee, F. S., Chu, Z. T., and Warshel, A. (1993) Microscopic and Semimicroscopic Calculations of Electrostatic Energies in Proteins by the POLARIS and ENZYMIX Programs, *J. Comput. Chem. 14*, 161−185.
23. Singh, U. C., and Kollman, P. A. (1984) An approach to computing electrostatic charges for molecules, *J. Comput. Chem. 5*, 129−145.
24. Frisch, M. J., Trucks, G. W., Schlegel, H. B., Scuseria, G. E., Robb, M. A., Cheeseman, J. R., Montgomery, J. A., Jr., Vreven, T., Kudin, K. N., Burant, J. C., Millam, J. M., Iyengar, S. S., Tomasi, J., Barone, V., Mennucci, B., Cossi, M., Scalmani, G., Rega, N., Petersson, G. A., Nakatsuji, H., Hada, M., Ehara, M., Toyota, K., Fukuda, R., Hasegawa, J., Ishida, M., Nakajima, T., Honda, Y., Kitao, O., Nakai, H., Klene, M., Li, X., Knox, J. E., Hratchian, H. P., Cross, J. B., Adamo, C., Jaramillo, J., Gomperts, R., Stratmann, R. E., Yazyev, O., Austin, A. J., Cammi, R., Pomelli, C., Ochterski, J. W., Ayala, P. Y., Morokuma, K., Voth, G. A., Salvador, P., Dannenberg, J. J., Zakrzewski, V. G., Dapprich, S., Daniels, A. D., Strain, M. C., Farkas, O., Malick, D. K., Rabuck, A. D., Raghavachari, K., Foresman, J. B., Ortiz, J. V., Cui, Q., Baboul, A. G., Clifford, S., Cioslowski, J., Stefanov, B. B., Liu, G., Liashenko, A., Piskorz, P., Komaromi, I., Martin, R. L., Fox, D. J., Keith, T., Al-Laham, M. A., Peng, C. Y., Nanayakkara, A., Challacombe, M., Gill, P. M. W., Johnson, B., Chen, W., Wong, M. W., Gonzalez, C., and Pople, J. A. (2003) *Gaussian '03*, Gaussian, Inc., Pittsburgh, PA.
25. Klamt, A., and Schuurmann, G. (1993) COSMO: A New Approach to Dielectric Screening in Solvents with Explicit Expressions for the Screening Energy and Its Gradient, *J. Chem. Soc., Perkin Trans. 2*, 799−805.
26. Barone, V., and Cossi, M. (1998) Quantum calculation of molecular energies and energy gradients in solution by a conductor solvent model, *J. Phys. Chem. A 102*, 1995−2001.
27. Langen, R., Brayer, G. D., Berghuis, A. M., McLendon, G., Sherman, F., and Warshel, A. (1992) Effect of the Asn52-Ile Mutation on the Redox Potential of Yeast Cytochrome *c*, *J. Mol. Biol. 224*, 589−600.
28. Olsson, M. H. M., Hong, G., and Warshel, A. (2003) Frozen Density Functional Free Energy Simulations of Redox Proteins: Computational Studies of the Reduction Potential of Plastocyanin and Rusticyanin, *J. Am. Chem. Soc. 125*, 5025−5039.
29. Warshel, A., Sussman, F., and King, G. (1986) Free Energy of Charges in Solvated Proteins: Microscopic Calculations Using a Reversible Charging Process, *Biochemistry 25*, 8368−8372.
30. Sham, Y. Y., Chu, Z. T., Tao, H., and Warshel, A. (2000) Examining Methods for Calculations of Binding Free Energies: LRA, LIE, PDLD-LRA, and PDLD/S-LRA Calculations of Ligands Binding to an HIV Protease, *Proteins: Struct., Funct., Genet. 39*, 393−407.
31. King, G., and Warshel, A. (1989) A Surface Constrained All-Atom Solvent Model for Effective Simulations of Polar Solutions, *J. Chem. Phys. 91*, 3647−3661.
32. Lee, F. S., Chu, Z. T., Bolger, M. B., and Warshel, A. (1992) Calculations of Antibody-Antigen Interactions: Microscopic and Semi-Microscopic Evaluation of the Free Energies of Binding of Phosphorylcholine Analogs to McPC603, *Protein Eng. 5*, 215−228.
33. Sham, Y. Y., and Warshel, A. (1998) The Surface Constrained All Atom Model Provides Size Independent Results in Calculations of Hydration Free Energies, *J. Chem. Phys. 109*, 7940−7944.
34. Alden, R. G., Parson, W. W., Chu, Z. T., and Warshel, A. (1995) Calculations of Electrostatic Energies in Photosynthetic Reaction Centers, *J. Am. Chem. Soc. 117*, 12284−12298.
35. Olsson, M. H. M., Parson, W. W., and Warshel, A. (2006) Dynamical Contributions to Enzyme Catalysis: Critical Tests of a Popular Hypothesis, *Chem. Rev. 106*, 1737−1756.
36. Olsson, M. H. M., Mavri, J., and Warshel, A. (2006) Transition state theory can be used in studies of enzyme catalysis: Lessons from simulations of tunnelling and dynamical effects in lipoxy-

genase and other systems, *Philos. Trans. R. Soc. London, Ser. B 361*, 1417−1432.
37. Warshel, A., and Papazyan, A. (1996) Energy Considerations Show that Low-Barrier Hydrogen Bonds Do Not Offer a Catalytic Advantage Over Ordinary Hydrogen Bonds, *Proc. Natl. Acad. Sci. U.S.A. 93*, 13665−13670.
38. Schutz, C. N., and Warshel, A. (2004) The low barrier hydrogen bond (LBHB) proposal revisited: The case of the Asp.His pair in serine proteases, *Proteins 55*, 711−723.
39. Mulholland, A. J., Lyne, P. D., and Karplus, M. (2000) Ab Initio QM/MM Study of the Citrate Synthase Mechanism. A Low-Barrier Hydrogen Bond Is not Involved, *J. Am. Chem. Soc. 122*, 534−535.
40. Molina, P. A., and Jensen, J. H. (2003) A predictive model of strong hydrogen bonding in proteins: The N-Δ^1-H-O-Δ^1 hydrogenbond in low-pH α-chymotrypsin and α-lytic protease, *J. Phys. Chem. B 107*, 6226−6233.
41. Shan, S. O., Loh, S., and Herschlag, D. (1996) The Energetics of Hydrogen Bonds in Model Systems: Implications For Enzymatic Catalysis, *Science 272*, 97−101.
42. Kim, K. S., Oh, K. S., and Lee, J. Y. (2000) Catalytic role of enzymes: Short strong H-bond-induced partial proton shuttles and charge redistributions, *Proc. Natl. Acad. Sci. U.S.A. 97*, 6373−6378.
43. Jencks, W. P. (1987) *Catalysis in Chemistry and Enzymology*, Dover, New York.
44. Villà, J., Strajbl, M., Glennon, T. M., Sham, Y. Y., Chu, Z. T., and Warshel, A. (2000) How important are entropic contributions to enzyme catalysis? *Proc. Natl. Acad. Sci. U.S.A. 97*, 11899−11904.
45. Warshel, A., and Parson, W. W. (2001) Dynamics of biochemical and biophysical reactions: Insight from computer simulations, *Q. Rev. Biophys. 34*, 563−670.
46. Zhang, X. Y., and Houk, K. N. (2005) Why enzymes are proficient catalysts: Beyond the Pauling paradigm, *Acc. Chem. Res. 38*, 379−385.
47. Pollack, S. J., Jacobs, J. W., and Schultz, P. G. (1986) Selective chemical catalysis by an antibody, *Science 234*, 1570−1573.
48. Tramontano, A., Janda, K. D., and Lerner, R. A. (1986) Catalytic antibodies, *Science 234*, 1566−1570.
49. Barbany, M., Gutierrez-de-Teran, H., Sanz, F., Villà-Freixa, J., and Warshel, A. (2003) On the Generation of Catalytic Antibodies by Transition State Analogues, *ChemBioChem 4*, 277−285.

BI061752U